



A Symmetric RuO₂/RuO₂ Supercapacitor Operating at 1.6 V by Using a Neutral Aqueous Electrolyte

Hui Xia,^{a,z} Ying Shirley Meng,^{b,*} Guoliang Yuan,^a Chong Cui,^a and Li Lu^{c,z}

^aSchool of Materials Science and Engineering, Nanjing University of Science and Technology, Nanjing, Jiangsu 210094, China

^bDepartment of NanoEngineering, University of California San Diego, La Jolla, California 92093-0448, USA

^cDepartment of Mechanical Engineering, National University of Singapore, 9 Engineering Drive 1, Singapore 117576

A novel symmetric RuO₂/RuO₂ supercapacitor with a high operating voltage of 1.6 V is built using the nanocrystalline hydrous RuO₂. The symmetric supercapacitor exhibits an energy density of 18.77 Wh kg⁻¹ at a power density of 500 W kg⁻¹ based on the total mass of active electrode material and excellent cycling stability and power capability. These results demonstrate the potentialities of using RuO₂ for symmetric supercapacitor or using RuO₂ as negative electrode for asymmetric supercapacitor with high energy density.

© 2012 The Electrochemical Society. [DOI: 10.1149/2.023204esl] All rights reserved.

Manuscript submitted October 12, 2011; revised manuscript received January 3, 2012. Published February 3, 2012.

Currently, most commercial supercapacitors are based on two symmetric activated carbon (AC) electrodes in organic electrolytes.^{1,2} The restriction of aqueous electrolytes is a limited operating voltage of about 1.23 V at which water decomposes. Although organic electrolytes usually can provide a high operating voltage up to 4 V, they have many disadvantages such as low ionic conductivity, high cost, tedious purification processes and flammability. On the contrary, aqueous electrolytes have merits in terms of high ionic conductivity, low cost, inflammability, and environmental benignity, which make the supercapacitors using aqueous electrolytes more attractive. To further improve the energy density of aqueous electrolyte-based supercapacitor, widening the voltage window is the key. One strategy is to select electrode materials that have high overpotentials for hydrogen and/or oxygen evolutions. Another one is to combine different positive and negative electrode materials that have well-separated potential windows to make asymmetric supercapacitors, enabling widening of the cell voltage.

Aqueous electrolyte-based asymmetric supercapacitors using AC as the negative electrode and various metal oxides/hydroxides or conducting polymers as the positive electrode are able to achieve a cell voltage of 1.4–2.0 V.^{3–8} Several studies indicated that metal oxides could also be used as negative electrodes in asymmetric supercapacitors.^{9–11} Among metal oxides, ruthenium oxide (RuO₂) has very high metallic conductivity and excellent supercapacitive performance with high specific capacitance.¹² It was found that RuO₂ has a high overpotential for oxygen evolution in acid solution.¹³ However, RuO₂ has a very low overpotential for hydrogen evolution in acid solution.¹⁴ Therefore, RuO₂ has rarely been studied as the negative electrode in aqueous electrolytes for asymmetrical supercapacitors. In this letter, a symmetric aqueous supercapacitor using RuO₂ as both negative and positive electrode is built, achieving a high operating voltage of 1.6 V with high energy density and power density. The supercapacitive performance of RuO₂ has rarely been reported in neutral aqueous electrolyte. Most importantly, a RuO₂/RuO₂ symmetric supercapacitor has been demonstrated using neutral aqueous electrolyte, which is different with most other RuO₂ reports that have only studied single electrode performance. To our best knowledge, this is the first time that a 1.6 V high voltage symmetric supercapacitor has been demonstrated by using the same metal oxide as two electrodes.

Experimental

Hydrous RuO₂ was prepared by a mild hydrothermal reaction. In a typical synthesis process, 0.1 g RuCl₃ · xH₂O (Alfa Aesar) was added to 25 mL distilled water. After mixing, the solution was transferred to

a 30 mL autoclave and heated at 180°C for 12 h in an electric oven for the hydrothermal reaction. The products were washed with deionized water and collected by centrifuge. The products were then dried in an electric oven at 70°C for 24 h.

The crystalline structure of the products was characterized by X-ray diffraction (XRD, Shimadzu X-ray diffractometer 6000, Cu-Kα radiation) with a scan rate of 2° min⁻¹. The nanostructure of RuO₂ was investigated by transmission electron microscopy (TEM) and high resolution transmission electron microscopy (HRTEM, JEOL, JEM-2010). To prepare the electrode, 80 wt% RuO₂, 10 wt% carbon black and 10 wt% polyvinylidene difluoride (PVDF) dissolved in N-methylpyrrolidone (NMP) were mixed to form a slurry. The slurry was pasted on Ti foil and dried in an electric oven at 70°C for 12 h. The loading of RuO₂ is about 0.4 mg for each electrode. The electrochemical test of individual RuO₂ electrode was performed using a three-electrode cell with a platinum foil counter electrode and an Ag/AgCl (saturated KCl) reference electrode. The symmetric RuO₂/RuO₂ system was investigated using Swagelok type two-electrode cells with a porous nonwoven cloth as the separator. For both three-electrode cell and two-electrode cell, 1 M Na₂SO₄ was used as the electrolyte. All electrochemical measurements were performed using a Solartron 1287 electrochemical interface.

Results and Discussion

Figure 1a shows the XRD pattern of hydrous RuO₂ synthesized by hydrothermal reaction. Three broad diffraction peaks in Figure 1 can be observed and indexed to a rutile RuO₂ phase (JCPDS 43-1027). The poor constructive diffractions are probably due to the nanocrystalline nature and the presence of defects (such as surface hydroxyl group) of hydrous RuO₂.^{15,16} The hydrous RuO₂ presents a fine-porous structure with continuous three-dimensional framework porosity as shown in the TEM image of Figure 1b. The HRTEM image of hydrous RuO₂ shown in Figure 1c indicates the formation of nanocrystalline with a particle size in the range of 2 ~ 3 nm.

Cyclic voltammograms (CVs) of RuO₂ electrode in various voltage windows in a three-electrode cell at a scan rate of 20 mV s⁻¹ are shown in Figure 2. As shown in Figure 2a, the CVs of the RuO₂ electrode exhibit similar rectangular shape in both negative window (-1 ~ 0 V vs. Ag/AgCl) and positive window (0 ~ 1 V vs. Ag/AgCl), indicating ideal capacitive behavior. For the positive window, a current leap at the positive end of the potential window, which increases as the upper potential limit increases from 0.8 to 1.0 V (vs. Ag/AgCl), is probably due to the oxygen evolution on the electrode. For the negative potential window, the current leap at the negative end of the potential window does not increase as the lower potential limit decreases, which probably indicates that the RuO₂ electrode has a high overpotential for hydrogen evolution. The specific capacitances of RuO₂ cal-

* Electrochemical Society Active Member.

^z E-mail: jasonxiahui@gmail.com and luli@nus.edu.sg

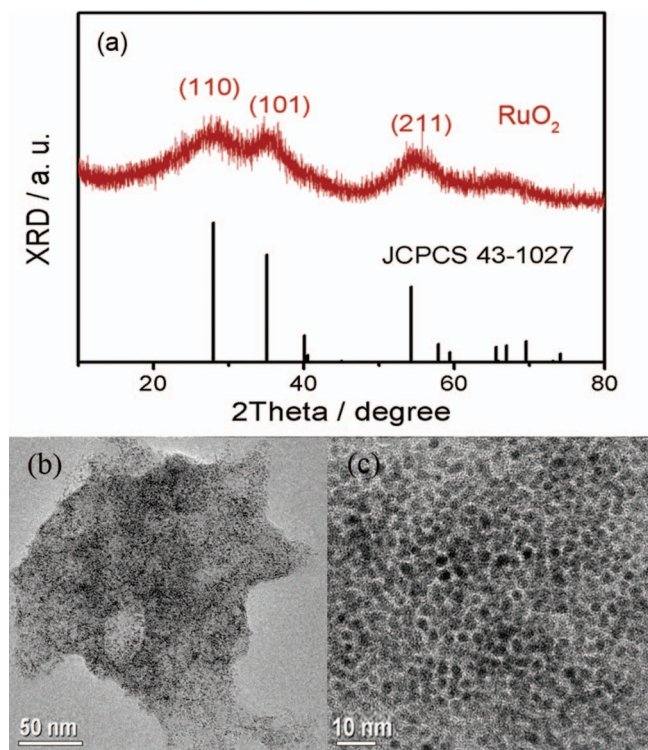


Figure 1. (a) XRD pattern of hydrous RuO₂ by hydrothermal method. (b) and (c) TEM images of hydrous RuO₂.

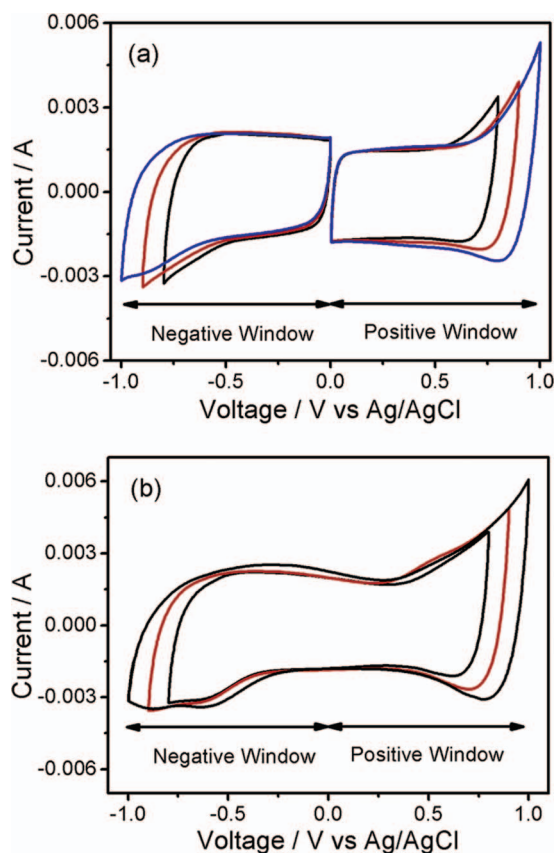


Figure 2. (a) CVs of RuO₂ electrode in various positive and negative windows. (b) CVs of RuO₂ electrode with different potential limits in continuous scan from negative window to positive window.

culated from the CVs for different potential windows are 205.9 F g⁻¹ (0–0.8 V), 209.6 F g⁻¹ (0–0.9 V), 231.1 F g⁻¹ (0–1 V), 228.2 F g⁻¹ (–0.8–0 V), 228.8 F g⁻¹ (–0.9–0 V), and 236.1 F g⁻¹ (–1–0 V), respectively. It is noticed that the specific capacitance of RuO₂ in a Na₂SO₄ electrolyte is lower than the value reported for RuO₂ in a H₂SO₄ electrolyte. Figure 2b shows the CVs of RuO₂ with different potential limits in continuous scan from negative window to positive window. It can be seen that RuO₂ has good electrochemical stability in a very broad potential window of about 2 V in Na₂SO₄ electrolyte. According to similar specific capacitances for both negative window and positive window, it is possible to make a symmetric supercapacitor using two RuO₂ electrodes.

The CVs of a symmetric RuO₂/RuO₂ supercapacitor with different potential windows at a scan rate of 20 mV s⁻¹ are shown in Figure 3a. For a low value of upper potential limit of 1.6 V, the CV exhibits a rectangular shape characteristic of a pure capacitive behavior. When the upper potential limit increases to 1.8 and 2.0 V, a current leap at the end of voltage window becomes obvious, which can be ascribed to gas evolution from positive electrode and/or the negative electrode. The potential-time curves of the individual positive electrode and negative electrode vs. the Ag/AgCl reference electrode and the potential-time curve of the full cell at a current of 1.5 mA are shown in Figure 3b. As shown in Figure 3b, when the full cell is charged between 0 and 1.6 V, the operating potential windows for the positive and negative electrode are [0.11; 0.91] and [0.11; –0.69] V vs. Ag/AgCl, respectively. It can be seen that the maximum cell voltage is limited by the positive electrode as the potential of positive electrode will exceed 0.91 V vs. Ag/AgCl when the full cell voltage increases to 1.8 or 2.0 V. As shown in Figure 2a, the irreversible oxidation of the positive electrode becomes obvious when the potential exceeds 0.9 V vs. Ag/AgCl. The successful demonstration of the high voltage symmetric RuO₂/RuO₂ supercapacitor could be attributed to high overpotentials for both hydrogen and oxygen evolutions of the nanocrystalline RuO₂ electrode in neutral electrolyte and the nanocrystalline feature of RuO₂. With

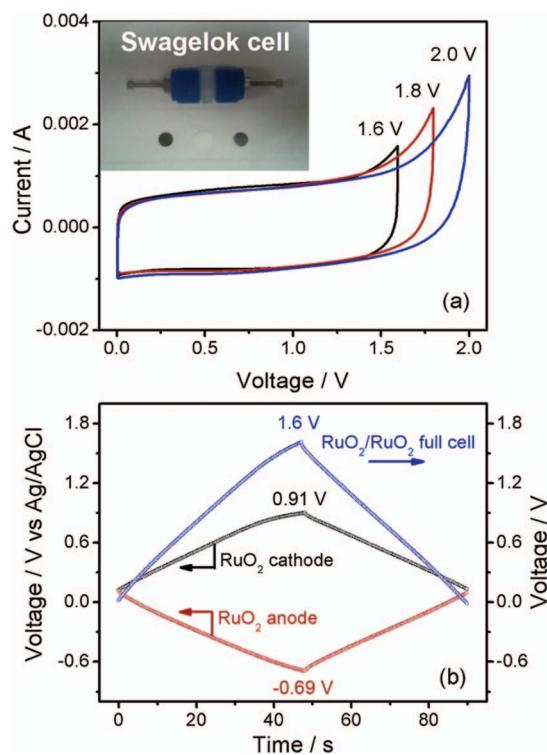


Figure 3. (a) The CVs of a symmetric RuO₂/RuO₂ supercapacitor with different potential windows. (b) The potential-time curves of the individual positive electrode and negative electrode vs. the Ag/AgCl reference electrode and the potential-time curve of the full cell at a current of 1.5 mA.

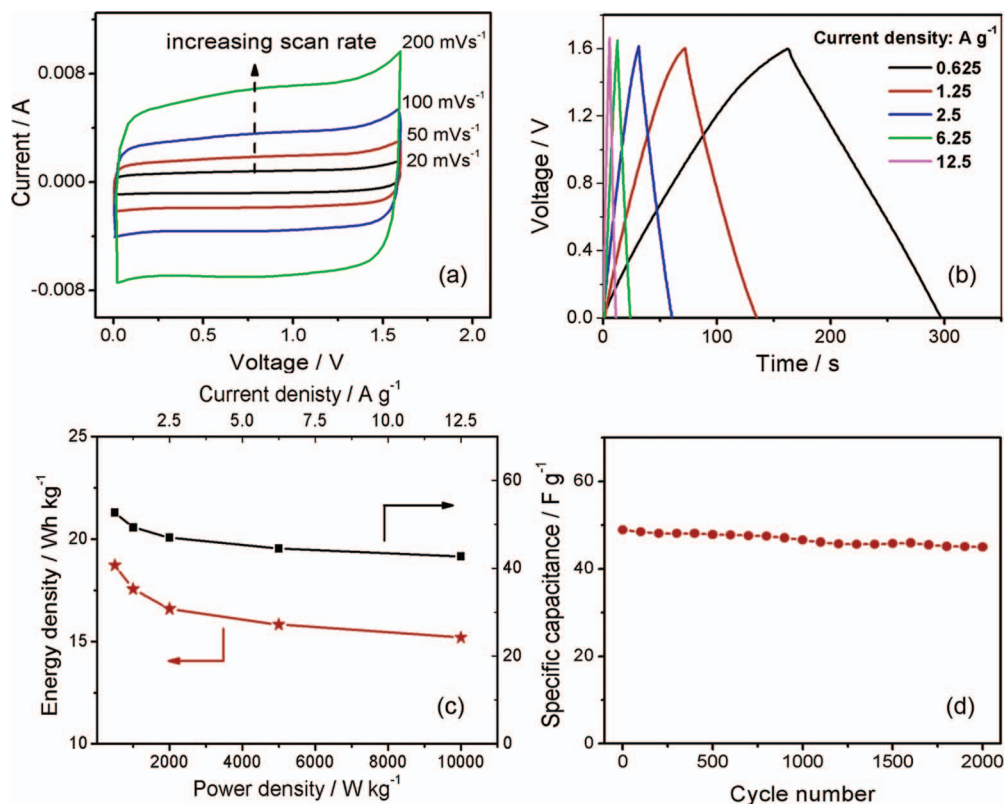


Figure 4. (a) The CVs of the symmetric RuO₂/RuO₂ supercapacitor between 0 and 1.6 V at different rates from 20 to 200 mV s⁻¹. (b) The galvanostatic charge/discharge curves of the symmetric supercapacitor at different current densities. (c) The specific capacitance of the symmetric supercapacitor as a function of current density and the Ragone plot of the full cell. (d) The cycle performance of the symmetric supercapacitor in the voltage window between 0 and 1.6 V at a current density of 2.5 A g⁻¹.

high overpotentials for both hydrogen and oxygen evolutions, the RuO₂ electrode can work in both negative and positive windows, thus leading to a high voltage for the full cell. In addition, the nanocrystalline feature of the RuO₂ electrode provides a large surface area with large and matched specific capacitances in both negative and positive windows, making a high voltage symmetric supercapacitor with large capacitance possible.

Figure 4a shows the CVs of the symmetric RuO₂/RuO₂ supercapacitor between 0 and 1.6 V at different rates from 20 to 200 mV s⁻¹. The cell maintains the rectangular shape of CVs even at a high scan rate of 200 mV s⁻¹, indicating ideal capacitive behavior and desirable fast charging/discharging property for power devices. The galvanostatic charge/discharge curves at different current densities, as shown in Figure 4b, reveal the linear voltage-time relation, characteristic of an electric double layer capacitance. The specific capacitance, C_s , of the full cell can be calculated from the charge/discharge curves according to the following equation:

$$C_s = \frac{I \times \Delta t}{\Delta V \times m} \quad [1]$$

where I is the current, Δt is the discharge time, ΔV is the potential window (1.6 V), and m is the total mass of RuO₂ from both positive and negative electrodes. The specific energy E_s and the specific power P_s can be calculated using the following equations:

$$E_s = \frac{I \Delta V \Delta t}{2m} \quad [2]$$

$$P_s = \frac{I \Delta V}{2m} \quad [3]$$

The specific capacitance as a function of current density and the Ragone plot of the full cell are shown in Figure 4c. The specific ca-

pacitance of the full cell reaches 52.66 F g⁻¹ at a current density of 0.625 A g⁻¹ and decreases to 42.73 F g⁻¹ at a current density of 12.5 A g⁻¹. The energy density of the symmetric supercapacitor is 18.77 Wh kg⁻¹ at a power density of 500 W kg⁻¹, which is higher than that of 1.6 V AC/AC symmetric supercapacitor (10 Wh kg⁻¹),¹⁷ and is comparable to that of asymmetric supercapacitors.^{3,9,10} Most importantly, the symmetric supercapacitor can deliver an energy density of 15.1 Wh kg⁻¹ at a high power density of 10 kW kg⁻¹, which makes it promising for high power applications. Moreover, the symmetric supercapacitor exhibits acceptable cycling stability in the voltage window between 0 and 1.6 V at a current density of 2.5 A g⁻¹ (Figure 4d). After 2000 cycles, the symmetric supercapacitor retains a high specific capacitance of 45 F g⁻¹, which is about the 92% of its initial capacitance.

Due to the high cost, RuO₂ itself may not be very promising in actual applications, but the exciting thing is that a high voltage symmetric supercapacitor can be made using neutral aqueous electrolyte and metal oxide electrodes. If this proof of concept works for RuO₂, it could also most likely work for other metal oxides with low cost, such as Co₃O₄, Fe₂O₃, SnO₂, and etc. It is expected that more people will explore the possibility of using other nanostructured metal oxides as electrodes to build high voltage symmetric or asymmetric supercapacitors in neutral aqueous electrolytes.

Conclusions

In summary, a symmetric supercapacitor has been built using hydroxide RuO₂ as both negative and positive electrodes with a high operating voltage of 1.6 V. The symmetric supercapacitor exhibits an energy density of 18.77 Wh kg⁻¹ at a power density of 500 W kg⁻¹ and an energy density of 15.1 Wh kg⁻¹ at a power density of 10 kW kg⁻¹. In addition to high energy density and power density, the

symmetric supercapacitor also exhibits good cycling stability with 92% of initial capacitance retained after 2000 cycles.

Acknowledgments

This research is supported by National Natural Science Foundation of China (No. 51102134), Nanjing University of Science and Technology through the research grant NUST Research Funding (2011ZDJH21 and AB41385).

References

1. P. Simon and Y. Gogotsi, *Nat. Mater.*, **7**, 845 (2008).
2. A. Burke, *Electrochim. Acta*, **53**, 1083 (2007).
3. Q. T. Qu, Y. Shi, S. Tian, Y. H. Chen, Y. P. Wu, and R. Holze, *J. Power Sources*, **194**, 1222 (2009).
4. Q. T. Qu, B. Wang, L. C. Yang, Y. Shi, S. Tian, and Y. P. Wu, *Electrochem. Commun.*, **10**, 1652 (2008).
5. Q. T. Qu, L. Li, S. Tian, W. L. Guo, Y. P. Wu, and R. Holze, *J. Power Sources*, **195**, 2789 (2010).
6. P. C. Gao, A. H. Lu, and W. C. Li, *J. Power Sources*, **196**, 4095 (2011).
7. Z. S. Wu, W. C. Ren, D. W. Wang, F. Li, B. L. Liu, and H. M. Cheng, *ACS Nano*, **4**, 5835 (2010).
8. Q. T. Qu, P. Zhang, B. Wang, Y. H. Chen, S. Tian, Y. P. Wu, and R. Holze, *J. Phys. Chem. C*, **113**, 14020 (2009).
9. K. C. Ng, S. W. Zhang, C. Peng, and G. Z. Chen, *J. Electrochem. Soc.*, **156**, A846 (2009).
10. P. C. Chen, G. Z. Shen, Y. Shi, H. T. Chen, and C. W. Zhou, *ACS Nano*, **4**, 4403 (2010).
11. W. Tang, L. L. Liu, S. Tian, L. Li, Y. B. Yue, Y. P. Wu, K. Zhu, *Chem. Commun.*, **47**, 10058 (2011).
12. T. S. Hyun, J. E. Kang, H. G. Kim, J. M. Hong, and I. D. Kim, *Electrochem. Solid-State Lett.*, **12**, A225 (2009).
13. T. C. Liu, W. G. Pell, and B. E. Conway, *Electrochim. Acta*, **42**, 3541 (1997).
14. T. C. Wen and C. C. Hu, *J. Electrochem. Soc.*, **139**, 2158 (1992).
15. K. H. Chang and C. C. Hu, *Appl. Phys. Lett.*, **88**, 193102 (2006).
16. K. H. Chang, C. C. Hu, and C. Y. Chou, *Chem. Mater.*, **19**, 2112 (2007).
17. B. Xu, F. Wu, R. J. Chen, G. P. Cao, S. Chen, G. Q. Wang, and Y. S. Yang, *J. Power Sources*, **158**, 773 (2006).